31st Congress of the International Council of the Aeronautical Sciences

Belo Horizonte, Brazil; September 09-14, 2018

RESULTS AND COMPARISON OF NUMERICAL SIMULATION AND THE TESTING OF LUG MANUFACTURED BY COMPOSITE MATERIAL BY RTM PROCESS

G. C. Fonseca[1]*, S.F.M. Almeida[2]

[1]Empresa Brasileira de Aeronáutica – Embraer – Centro de Engenharia e Tecnologia, Minas Gerais, Brasil

[2]Instituto Tecnológico de Aeronáutica - ITA, São José dos Campos, Brasil

Keywords: *resin transfer molding, thick laminate, material composite, finite element method*

Abstract

The focuses of this work are comparison between the numerical simulation and the testing of lug manufactured by composite material by RTM process and using manufacturing methodology of thick composite laminated components for aeronautical applications. This work proposes to develop a finite element method numerical simulations and the manufacturing of a composite lug material by resin transfer molding (RTM). The following points were accomplished: the design and manufacture of mechanisms for testing, the instrumentation of test specimens - lugs (named as SPC), the methodology of data acquisition and analysis of results obtained. In the numerical part in the first instance, held a simplified analysis of the specimen using finite elements, in order to define an optimal thickness to a value established by pre-loading envelope of aircraft loads. Subsequently, a series of numerical analysis was performed by simulating the initiation and propagation of cracks and, consequently, the structural failure of the component.

1 Introduction

The aviation industry has always been in a constant search of structural design improvement and on the development of components that would result in greater reliability. Studies have shown that when one correlates material properties and manufacturing process it is possible to obtain enormous productivity gains, quality increase and considerable costs reduction. This work is intended to determine using finite element method modeling, the composite laminates, manufactured by RTM method, optimum thickness under a specific loading conditions. The numerical analysis methodology made use of finite element method with *Abaqus 6.10-1*. Studies about thick composite laminates can significantly contribute on the process of manufacturing structural components. Those components can replace metallic materials that are currently used. Manufacturing process improvement can also generate great benefits, because it can reduces industrial costs and manufacturing time, besides structural weight reduction resulting in better aircraft performance. By the method proposed, only one mold can manufacture many lugs, ensuring manufacturing reproduction and avoiding finishing process. The results obtained in this work can also contribute for better comprehension of thick composite laminates manufacturing for practical application on the aeronautical industry.

2 Methodology

The study can be divided in two parts: **1st. part).** Design and manufacture of mechanisms for testing, the instrumentation of test specimens (lugs), methodology of data acquisition, and analysis of results obtained. **2nd. Part).** In the numerical part in the first instance, held a simplified analysis of the specimen using finite elements, in order to define an optimal thickness to a value established by pre-loading envelope of aircraft loads. Subsequently, a series of numerical analysis was performed by simulating the initiation and propagation of cracks and, consequently, the structural failure of the component.

3 Results

3.1 Structural element – lug

The lug geometry was studied by observing various applications in structural assemblies to which associated a similarity with the objectives of this project. This structural element may be used in the connection between the horizontal stabilizer and the fuselage and it´s responsible for load transfer between these parts of the aircraft.

According to Fonseca *et al* [1] the geometry of the lug, looking for associate the mold manufacturing processes and parts and perform the test, that will be analyze on this paper as shown in Fig. 1.

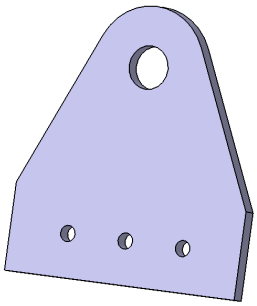

Figure 1. Isometric view of final lug design.

As required forty-eight layers are required to meet the proposed requirements for loading and failure specimen according to results of the numerical analysis. As required forty-eight layers are required to meet the proposed requirements for loading and failure specimen according to results of the previous numerical analysis. These layers are arranged in the specimen modeling in the following order in Eq. (1):

$$[+45, -45, 0, 90, 90, 0, -45, +45]_{6T} \quad (1)$$

The first simulation and result obtained in the finite element model as shown in Fig. 2 and will be used for next steps.

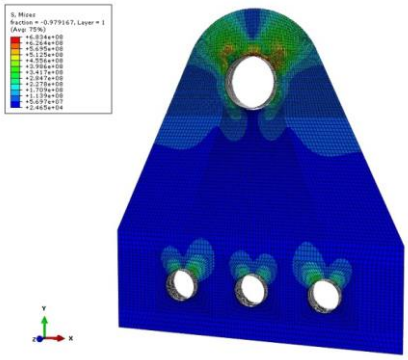

Figure 2. Finite elements results for general geometry.

3.2 Lug Topology

With the lug topology defined according to criteria of manufacture and failure region, determines the values of geometric element measured. The lug is manufactured according to measurements shown in Fig. 3:

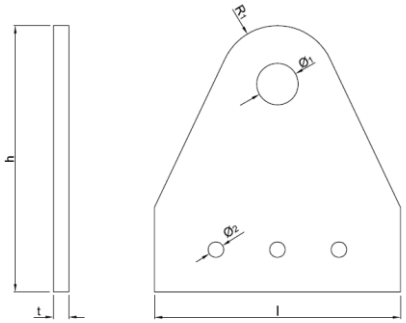

Figure 3. Lug Topology.

Where: t – thickness
l – width
h – height
R_1 – radius of lug
ϕ_1 – pin diameter
ϕ_2 – bolts diameter (typical – 3x)

The dimensions listed above are shown in Tab. 1.

Table 1. Basic dimensions of lug

Parameter	Dimension (mm)
t	11,76
h	200
l	190
ϕ_1	32
ϕ_2	12
R_1	45

More details about manufacturing, measure of characteristics, drilling and finishing process of specimens can be obtained on Fonseca *et al* [1]. After the drilling process and before preparation for the test, the specimens were as shown on Fig. 4:

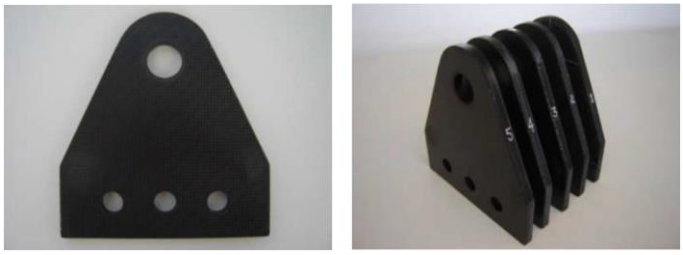

Figure 4. Specimens prepared for instrumentation.

4. Preparing of specimens

4.1 Instrumentation of specimens

The strain gauges were positioned on one of the faces of specimens for obtain the strain zone during the application of the load in the test. Two axes reference were drawn to define the correct positioning, obeying the pre-defined location. Two strain gauges were attached in each specimen, in one axis of application of the load (0°) and another at 45° of this axis, being numbered respectively as EX-1 and EX-2, according to Fig. 5.

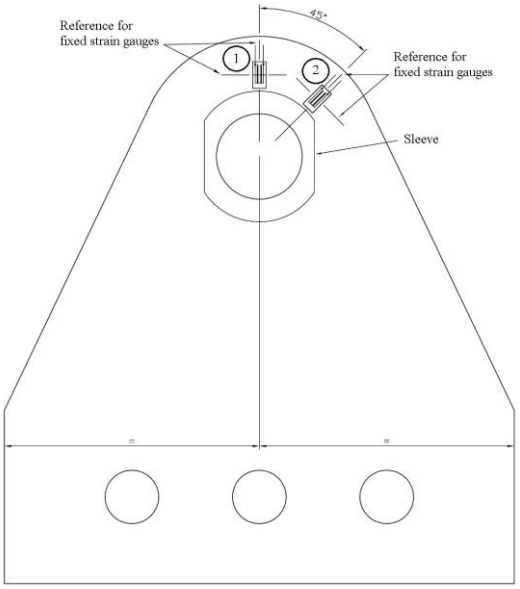

Figure 5. Positioning of strain gauges on specimens

With these strain gauges it will be possible to validate the strain zone on specimens and the values it will be comparing obtained with the numerical model. The Fig. 6 shows the region prepared and marked for install strain gauges installed after marked with the references and prepared.

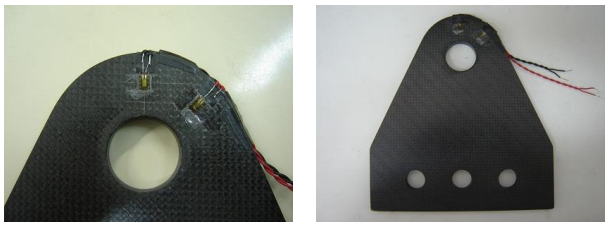

Figure 6. Strain gauges attached on position test with cables installed.

5. Implementation test

5.1 Test device

The test devices were designed with the purpose of obtaining a resultant load of traction on the axis of symmetry of the specimens. Some important points in the design of devices were considered, such as: costs, manufacturing feasibility and safety. The test devices referred to as the "test assembly" are shown in Fig. 7.

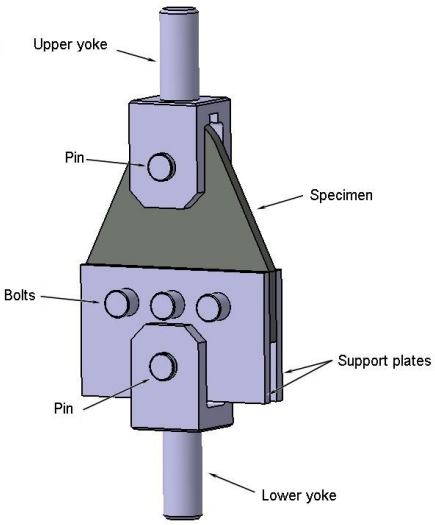

Figure 7. Design of test assembly.

All components of the test assembly were analyzed so as not to fail together with the test object, which is the test specimen. An

important assembly item that is the sleeve where the pin of the traction machine has been mounted is shown in Fig. 8 before being assembled in the test assembly.

Figure 8. Manufacturing sleeves.

5.2 Test Methodology

Assembly all parts for test

The final assembly for test specimen as show on Fig.9 below:

Figure 9. Assembly test specimen.

This assembly (support plates, yokes, sleeve, pin and bolts) on the traction machine for test as show on Fig. 10.

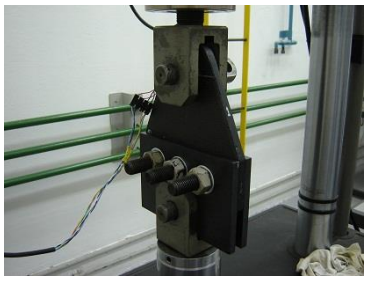

Figure 10. Assembly test specimen attached to test machine.

System of application load

For the test, an MTS traction machine model 810 - Material Test System was used with a load cell with a capacity of 250 kN. The machine uses a computer and a controller to apply the test parameters, as shown in Fig. 11.

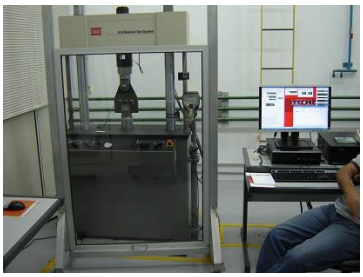

Figure 11. Traction machine uses on test specimen.

System Setup

Before carrying out the tests, it is necessary to inform the test parameters that will be used in the data acquisition interface for the extensometer, and in the load application interface referring to the traction machine. The data acquisition system was configured with the parameters of the extensometer, which are described below:

- minimum strain value: -20 micro strain
- maximum srain value: 20 micro strain
- gauge factor - 2.02 ± 1%
- resistance - 350 Ω
- configuration type - one quarter of “bridge”
- acquisition mode - continuous
- data acquisition frequency - 1 kHz

The strain gauges used are from the manufacturer HBM model 3/350LY11 and the parameters are on the manufacturer's sheet, supplied with them.

Load application speed

Kassapoglou *et al.* [3], carried out tests on test specimen loading them to the fault with nominal load interval values of 8.9 kN load. When audible damage occurred, the test was temporarily suspended for visual inspection. At the end of each load interval, the test was stopped and the test specimen was monitored for the previously applied load range, seeking edge delamination, pin damage, or other forms of visible or audible damage. Each charge value versus audible damage was noted during each test.

Wallin *et al.* [2], carried out tests on test specimens loading gradually, i.e. the load was added with 10-20 kN intervals and the strain was measured at each corresponding point.

Ahn *et al.* [4], performed tests on composite specimens made of unidirectional tape evaluating the loading in the bore. The loading was applied through a steel pin through the hole, with a loading speed of 1 mm/min.

Tong [5] performed bolt joints with bearing failures, and in the test specimens the speed of displacement of the upper claw of the machine was controlled by applying a constant displacement of 0.5 mm/min.

According to ASTM D 3039 [7], for standard tests of tensile strength, modulus of elasticity and Poisson's coefficient in composite laminates, the value of the nominal displacement velocity is a maximum of 1.27mm/min (0.05 in/min).

Standard ASTM D 5766 [6] defines, for test specimens made of composite laminate with a center hole, the value of the nominal displacement velocity of not more than 1.27 mm/min (0.05 in / min) in the standard tests to obtain the tensile strength and modulus of elasticity. In this way, the displacement velocity of 0.5 mm / min will be adopted, according to the citations and the test standards, being conservative in the load application value. In the displacement application interface referring to the tensile machine, the displacement velocity value was inserted according to each test described in Tab. 2.

Table 2. Load applied velocity adopted on tests.

	SPC 1	SPC 2	SPC 3	SPC 4	SPC 5
Test speed (mm/min)	0,5	1,0	0,5	0,5	0,5

The maximum displacement value during the test was determined to be 10 mm. The data acquisition system was developed in the *LabView* software with the *DAQmx* programming language, in the block diagram scheme. More details see Fonseca [11].

Test performing

Prior to any load application to the traction machine, a bulkhead was positioned in front of the machine to prevent projection of shrapnel specimens during the test. A preload according to Tab.3 was applied to the system in order to remove any gaps that may exist in the assembly of the parts. Subsequently the load and displacement were zeroed and the test started.

Table 3. Test specimens pre-load values.

	SPC 1	SPC 2	SPC 3	SPC 4	SPC 5
Pre-load (N)	200	10.000	10.000	10.000	10.000

The displacement is applied with constant velocity according to the predetermined value. It is monitored in real time in the interface screen shown above, and when a drop of more than 30% occurs at the maximum value of the load, the specimen failure is indicated, the application of the displacement is interrupted at the end of the test. After failure criteria, the load was withdrawn on the traction machine and the situation of the test specimen was analyzed after each test. The results can be seen in section "Results of the experimental tests of the specimens".

6. Analyzes of lug resistance with numerical method – finite element models

6.1 Modeling

The software used to develop the finite element models of this work was *Abaqus 6.10-1*. The quasi-static type of analysis was used in the steps of this study with the "Dynamic, Explicit" procedure to determine the load and collapse strains of the studied component. This module called *Abaqus/Explicit* uses the solution methodology called dynamic relaxation, detailed later.

6.2 Contact Mechanisms

The *Abaqus/Explicit* module provides two algorithms for contact modeling and interaction mechanisms: the general (automatic) contact algorithm and the peer contact algorithm. Fig. 12 illustrates the two forms of contact in the module:

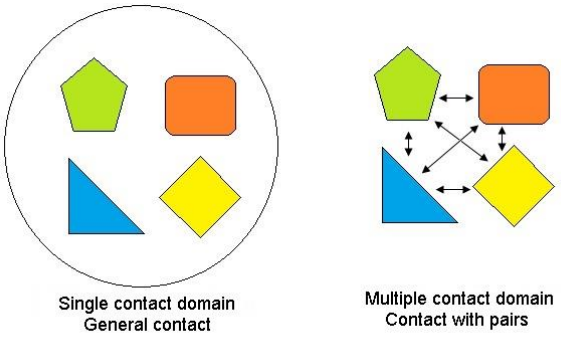

Figure 12. Types of algorithm for contact modeling.

The general contact algorithm of this module allows simple definitions and with few restrictions for the types of surface involved in the modeling according to *Abaqus* [10].

6.3 Formulation of the failure model

To solve the problem, the failure and degradation model was used, which detects the beginning and the propagation of damage, modifying the mechanical properties of the material in the affected area until the catastrophic failure of the element. The failure and degradation model was implemented in *Abaqus 6.10-1*, using the VUMAT (*User Defined Material Model*) routine. The model used in the solution of the problem was based on the work developed by Yokoyama *et al* [8] and Donadon *et al* [9].

6.4 Description of finite element models

The starting point of the numerical models was the definition of a structural component for aeronautical application. A single parameter has been defined at this point, which is the load that the component must support without crashing. It will be necessary to study several parameters of this component and later define the basic geometry. These changes in geometry will be mainly motivated by the results obtained in the analysis of finite elements of the models elaborated and evolved according to the results obtained. The flowchart of the general procedure proposed for the definition of the geometric parameters of the specimen and the evolution of the results according to numerical models and obtains the value of the component failure load, as developed in Fonseca [11]. The Fig. 13 represents the hybrid model with the mesh and the boundary conditions.

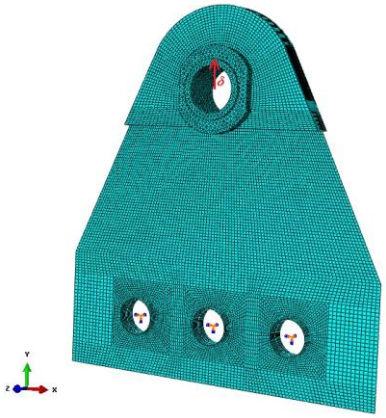

Figure 13. Hybrid model, boundary conditions and mesh used in modeling the problem.

In this model was simulated the non-linear condition according to the "Explicit Method - Dynamic Relaxation", using the failure model, according to mentioned in "Formulation of the failure model" implemented in *Fortran* software. With this analysis the catastrophic failure of the definitive geometry was evaluated, using the hybrid model, as previously mentioned. The results of this model are presented in the section "Results of analyzes obtained by finite element method".

7. Results

7.1 Results of experimental specimen test and numerical analysis of models

The results of the work will be analyzed in two parts. In the experimental part, it will be presenting the specimen response in the traction test obtaining the load x displacement and load x strain curves until the component rupture, resulting from the tensile machine and strain gauge measurements, respectively. In the numerical part, the results of the finite element model will be analyzed, comparing the values of failure load and strain with the data obtained experimentally.

7.2 Results of experimental specimen tests

The experimental results can be separated into two parts. The first part is the results of applying the load until the component fails, obtaining the failure load values for each specimen. These values are presented graphically through load x displacement curves, grouping the results for the five specimens tested. The second part are the values of the strain field obtained through the strain gauges positioned at 0° and 45° of the axis of application of the load, as showed in section "Instrumentation of test specimens". With this data, the load x strain curves are compiled by grouping the results for the five specimens tested.

Obtaining values of load failure for test specimens

The test load failure was obtained at the point where the highest load value is shown. The component failure was determined when a drop of more than 30% of the highest loading value occurred during the test. The values obtained in the load failure test are described in the Tab. 4.

Table 4. Values of load failure for test specimens.

	SPC 1	SPC 2	SPC 3	SPC 4	SPC 5
Load failure (kN)	126,1	154,9	141,3	139,7	149,2

In Fig. 14 the load x displacement curves are plotted. The displacement refers to the upper yoke of the test machine.

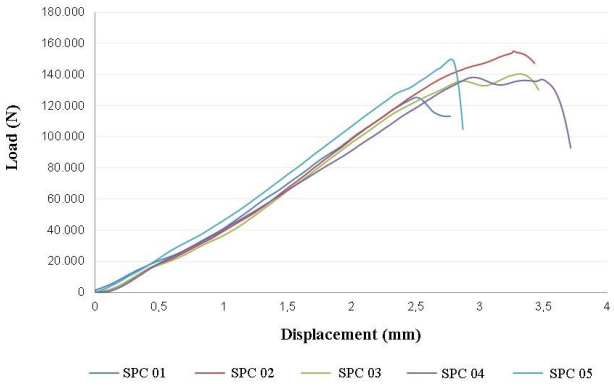

Figure 14. Load x displacement test curve.

In Fig. 15 are showed results of load x strain grouped for all the specimen tests with the strain gauge at 45°.

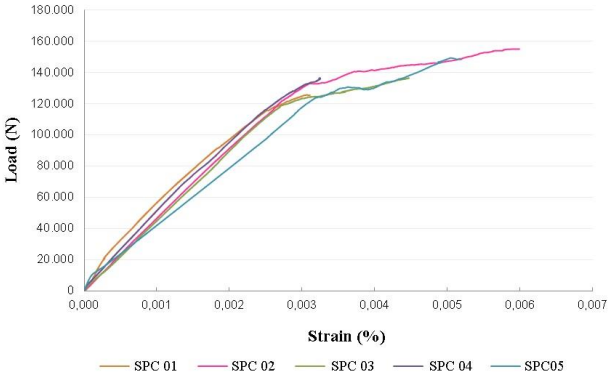

Figure 15. Results of load x strain grouped for all the specimen tests with the strain gauge at 45°.

Through this figure can observe a good repeatability of the results obtained in the tests. The curves didn´t present a very large dispersion and could obtain a typical stiffness value for the specimens. It is observed from the previous results that the nonlinearity occurs from the load value of 117 kN, or typically close to that value in all the tests. In Fig. 16 are showed results of load x strain grouped for all the specimen tests with the strain gauge at 0°. The strain gauge fixed at 0° at specimen 01 didn´t present consistent results, and it was concluded that the adhesive failed during bonding at that point. This value will be disregarded and won't be presented in the comparison of results with other specimens.

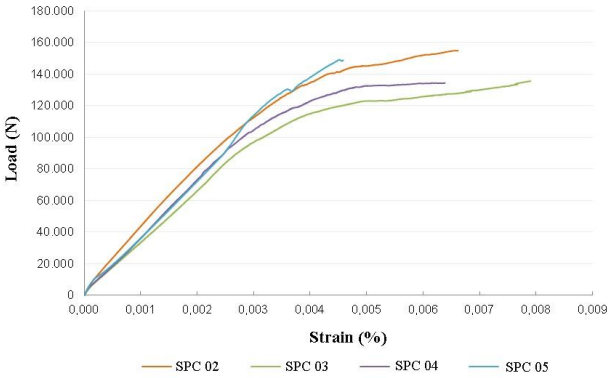

Figure 16. Results of load x strain grouped for all the specimen tests with the strain gauge at 0°.

Thus, all the specimens test results can be grouped verifying that the values didn´t present a very high dispersion. The curves didn´t present a very large dispersion and can

obtain a typical rigidity value for the specimens, as can be observed in Fig. 16. It can be observed that non-linearity occurs from the load value of 105 kN to 130 kN, presenting a greater dispersion in relation to the results of the strain gauges positioned at 45°.

7.3 Results of analysis obtained by finite element method

Results of analysis for lug resistance (failure load)

The load x displacement curve obtained from the proposed numerical model is shown in Fig. 17, where the behavior of the lug is represented until the catastrophic failure.

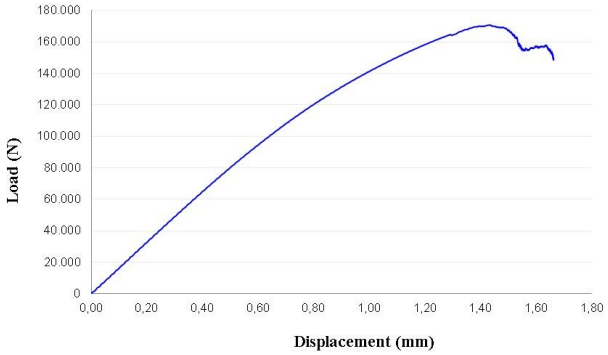

Figure 17. Results of load x displacement curve for numerical model.

According to the Fig. 17, it can be seen that the modeling of the test using optimum loading and boundary conditions results in an artificial failure load greater than the test failure load. The result obtained for the failure load is 170.8 kN.

Strain of the finite element model

The analysis of the strain was done by selecting elements of the finite element model corresponding to the points where the strain gauges were fixed at the two predefined points in the specimen. In this way the output curves with the values of strains ε_x and ε_y as a function of the applied load corresponding to the two points of the specimen will be obtained. The strains obtained from the finite element model are oriented according to the local reference system of each layer. In the model studied, the outer layer of the specimen is oriented at 45° with respect to its longitudinal axis. Thus, the values of the numerically obtained strains are associated with a rotated reference system of 45°. On this layer the value of ε_x, corresponding to the strain gauge located at 45° of the longitudinal axis will be obtained. In the model studied, the third layer outside the specimen is oriented at 0° in relation to its longitudinal axis. Thus, the values of the strains obtained numerically are associated with a rotated reference system of 0°. In this layer the value of ε_y, corresponding to the strain gauge located at 0° of the longitudinal axis, will be obtained. It is worth mentioning that the 0° oriented strain gauge of the longitudinal axis is fixed to the outermost layer of the specimen, by a data manipulation facility, the results were obtained in the third layer of the model oriented at 0° of the longitudinal axis. The results of strains obtained with finite element model on 0° (ε_y) and 45° (ε_x) as show in Fig. 18.

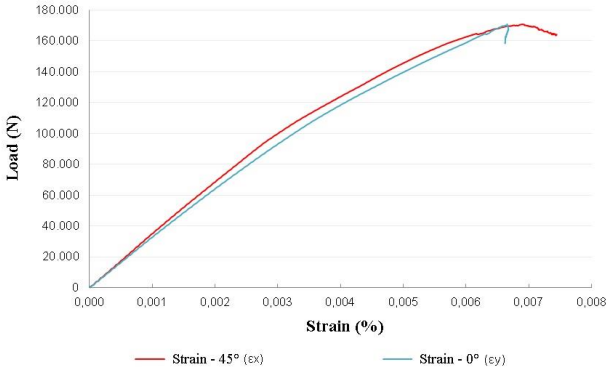

Figure 18. Strains obtained of finite element models on 45° (ε_x) and 0° (ε_y).

7.4 Comparison of the experimental results with the results obtained using the finite element method

The results obtained in the finite element models are compared with the results obtained in the experimental test in each case, and are separated by different figures to facilitate the comparison of the results. The strain results obtained in the test specimens and in the finite element model according to the strain gauge positioned at 45° (FEM 45°) from the longitudinal axis is shown in Fig. 19.

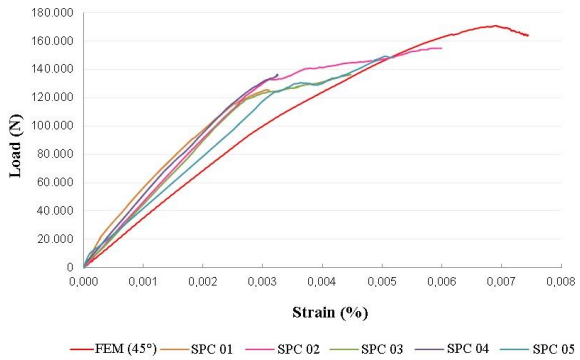

Figure 19. Strains of finite element model (FEM 45°) and results of test specimens (CDP´s).

The strain results obtained in the test specimens and in the finite element model according to the strain gauge positioned at 0° (FEM 0°) from the longitudinal axis is shown in Fig. 20.

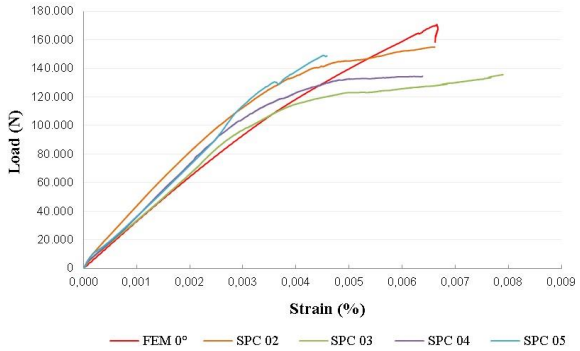

Figure 20. Strains of finite element model (FEM 0°) and results of test specimens (CDP´s).

7.5 Model calibration

The best correlation observed between the strain values measured in the test and those obtained from the analysis of the finite element model for the strain gauges positioned at 0° and 45° of the longitudinal axis is the results of specimen 03 (SPC 03) and specimen 05 (SPC 05) tested, respectively. For specimen 05, the accommodation effect of the test set should be disregarded for loads below 10 kN. In Fig. 29 this effect was corrected; removing the accommodation from the beginning of the curve, and the modified graph was compared with the results obtained in the finite element model. This correlation is valid for low load levels in both cases, because when the finite element model reaches higher load levels, the values obtained diverge due to nonlinear characteristics of the model. Comparing the inclination of the curves, a similarity between the results of the finite element model and the specimen tests is observed. This inclination represents stiffness in both cases. These comparisons of results can be observed in Fig. 21 and Fig. 22.

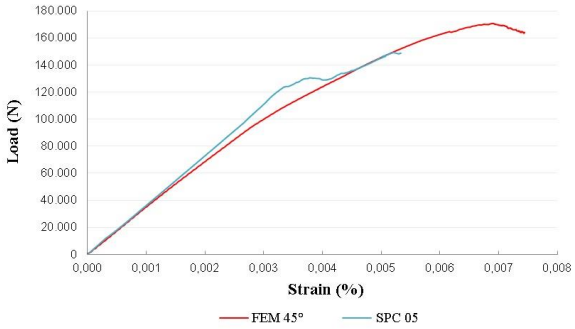

Figure 21. Comparasion between strains obtained on finite element model (FEM 45°) and test specimen (SPC 05).

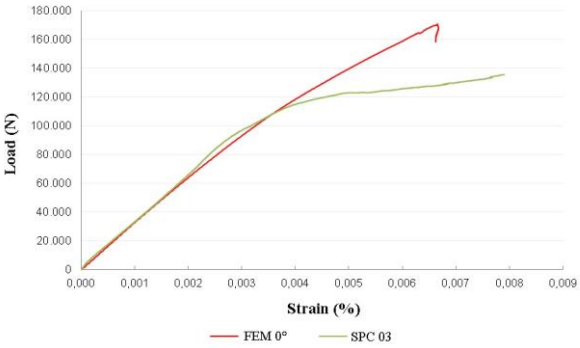

Figure 22. Comparasion between strains obtained on finite element model (FEM 0°) and test specimen (SPC 03).

8. Conclusions

From the point of view of the specimen test, it was possible to prove what had been predicted in the finite element model and characterize the behavior of this structural element during the test. Within the set of specimens, four tests presented failure load values with small dispersion. Only in the first test in which the sleeve failed, the value of the failure load was below the others, being influenced by this effect. The catastrophic failure of specimens was the same in the first four tests, but one first test occurred differently from the others. In the fifth test the failure occurred in every upper section of the specimen.

During the performance of the tests, the influence of increasing the speed load application for the second test was observed. The value of the failure load in this test was higher than the others, although the variation was not very high. Visually the failure of the second specimen also presented different from the other tests.

The objectives of the numerical part of this work were reached as proposed. The model was able to represent the behavior of the composite material subjected to the tensile load, obtaining the value of the failure load and its failure modes, comparing the numerical results with the results obtained in the experimental tests of the five specimens. The numerical analyses were separated into two parts. In the first part, it analyzed only the component failure load. In the second part, the results concerning localized deformation were analyzed, being possible to compare the stiffness values of the model and of the tests through the curves of load x strain. From the point of view of the failure load of the component, the result obtained in the finite element model was higher than the results obtained experimentally. This variation is due to the fact that it is not possible to achieve optimum boundary conditions defined in the finite element model. With respect to localized deformations, the results obtained in the finite element model were very close when compared to the test results. In the selected cases cited in section "Model calibration", a similarity was observed between the two results, limiting to some extent point of the test. With this, a reasonable approximation of the stiffness of the numerical model was observed compared to the stiffness obtained in the test of the manufactured specimens. The failure routine used in the model demonstrated robustness according to the proposed objective, since the results of the numerical model presented results related to failure very close to the results obtained in the experimental tests.

9. References

[1] Fonseca G. C., and Almeida S. F. M., **Numerical Simulation in Finite Element Method and Manufacturing of Lug Material Composite by RTM Process**, 30th Congress of International Council of the Aeronautical Sciences, September 2016.

[2] Wallin, M., Saarela, O., Law, B., Liehu, T., **RTM Composite Lugs for High Load Transfer Applications,** 25th International Congress Of the Aeronautical Sciences, September 2006.

[3] Kassapoglu, C., Townsend JR., W. A., **Failure Prediction of Composite Lugs Under Axial Loads,** AIAA Journal, V. 41, n. 11, November 2003.

[4] Ahn, H.-S., Kweon, J.-H., Choi, J.-H., **Failure of Unidirectional-Woven Composite Laminated Pin-Loaded**, Journal of Reinforced Plastics and Composites, 2005.

[5] Tong, L., Bearing Failure of Composite Bolted Joints with Non-Uniform Bolt-to-Washer Clearance, Composites: Part A, v. 31, p. 609–615, 2000.

[6] ASTM D 5766/D 5766M, Standard Test Method for Open-Hole Tensile Strength of Polymer Matrix Composite Laminates, 2011.

[7] ASTM D 3039/D 3039M, Standard Test Method for Tensile Properties of Polymer Matrix Composite Materials, 2008.

[8] Yokoyama, N. O., Donadon, M. V., Almeida, S. F. M, A numerical study on the impact resistance of composite shells using an energy based failure model. 2010 (submetido para publicação).

[9] Donadon, M. V., Almeida, S. F. M., Faria A. R., Arbelo, M. A., **A Three-Dimensional Ply Failure Model for Composite Structures.** International Journal of Aerospace Engineering, 2009, doi: 10.1155/2009/486063.

[10] ABAQUS 6.10-1. Theory manual, 2010.

[11] Fonseca G. C., **Simulação Numérica em Elementos Finitos, Fabricação e Ensaio Experimental de um Olhal em Material Compósito**. 2012. 233f. Tese de Mestrado – Área de Mecânica dos Sólidos e Estruturas – Instituto Tecnológico de Aeronáutica, São José dos Campos.

Contact Author Email Address

giovane.fonseca@embraer.com.br
giovane@ufmg.br

Copyright Statement